



DIE  
TI.

UNI  
NA

VERSITA' DEGLI STUDI DI  
POLI FEDERICO II

DIPARTIMENTO DI INGEGNERIA ELETTRICA  
E DELLE TECNOLOGIE DELL'INFORMAZIONE

**Michela Gravina\***, Diego Gragnaniello\*, Luisa Verdoliva†, Giovanni Poggi\*, Iuri Corsini§, Carlo Dani§, Fabio Meneghin¶, Gianluca Lista¶, Salvatore Aversall, Francesco Raimondi‡, Fiorella Migliaro‡ and Carlo Sansone\*

\*Dept. of Electrical Eng. and Information Technology, University of Naples Federico II, Naples, Italy

†Dept. of Industrial Engineering, University of Naples Federico II, Naples, Italy

‡Division of Neonatology, Section of Pediatrics, Dept. of Translational Medical Sciences, University of Naples Federico II, Naples, Italy

§Hospital Careggi of Florence, Italy

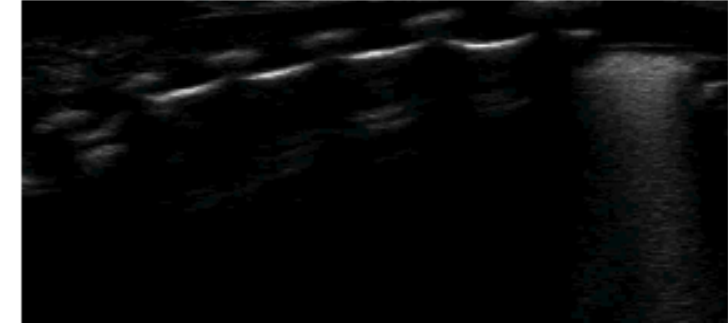
¶Hospital "Vittore Buzzi", Milan, Italy

||Civil Hospital of Brescia, Italy

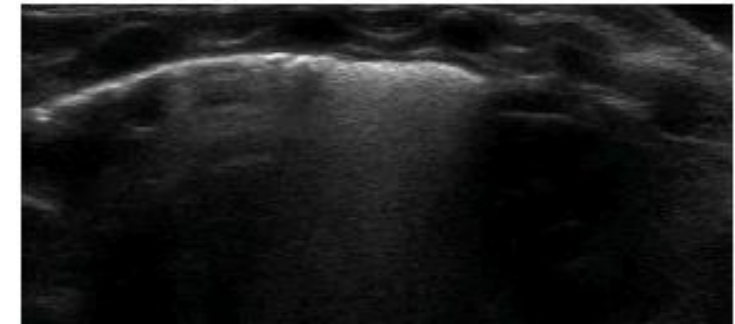
# Deep learning in the ultrasound evaluation of neonatal respiratory status

# Lung Ultrasound Advantages

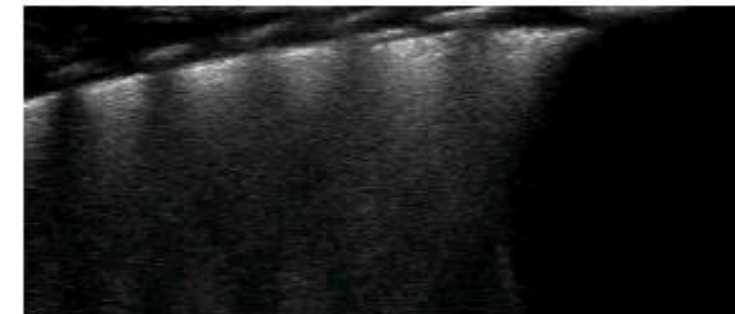
- Lung Ultrasound (US) for neonatal respiratory status evaluation:
  - ✓ Exhibits a high descriptive power
  - ✓ Is able to analyze anatomical structures, like pleural line and artifacts, exploited by experts to assess the lung composition and status
  - ✓ Provides a visual assessment of the respiratory status of newborn patients
  - ✓ Reveals the need for respiratory support
  - ✓ Is a harmless technique, compared to the standard X-rays (RX)
- **US images are prone to many investigations through either visual inspection or computer-aided analysis**



Healthy



Transient Tachypnea of the Newborn (TTN)



Respiratory Distress Syndrome (RDS)

# Lung Ultrasound for Neonatal Respiratory Status

- Several studies have focused their attention on fetal lung US image analysis.

Authors	Approach	Analysis
<sup>1</sup> A. Perez-Moreno et al.	textural descriptors	respiratory status
<sup>2</sup> Y. Du et al.	textural descriptors	respiratory status
<sup>3</sup> M. K. Abdelhamid et al	textural descriptors	newborn diseases prediction
<sup>4</sup> M. Palacio et al.	textural descriptors	respiratory morbidity
<sup>5</sup> P. Chen et al.	fully automatic	neonatal maturation degree prediction
<sup>6</sup> X. P. Burgos-Artizzu et al.	fully automatic	respiratory morbidity
<sup>7</sup> F. Raimondi et al.	texture analysis	respiratory status

- The proposed work:
  - Exploits Deep Learning (DL) approaches to define a score directly obtained from US images
  - Tests its correlation with pulse oximetric saturation ratio  $SpO_2/FiO_2$  (SF)
  - Analyzes the performance of recent state-of-art Convolutional Neural Networks (CNNs)

<sup>1</sup>A. Perez-Moreno et al. "Clinical feasibility of quantitative ultrasound texture analysis: A robustness study using fetal lung ultrasound images," Journal of Ultrasound in Medicine

<sup>2</sup>Y. Du et al. "Application of ultrasound-based radiomics technology in fetal lung texture analysis in pregnancies complicated by gestational diabetes or pre-eclampsia," Ultrasound in Obstetrics & Gynecology, 2020.

<sup>3</sup>M. K. Abdelhamid et al. "Quantitative Ultrasound Texture Analysis of Fetal Lung

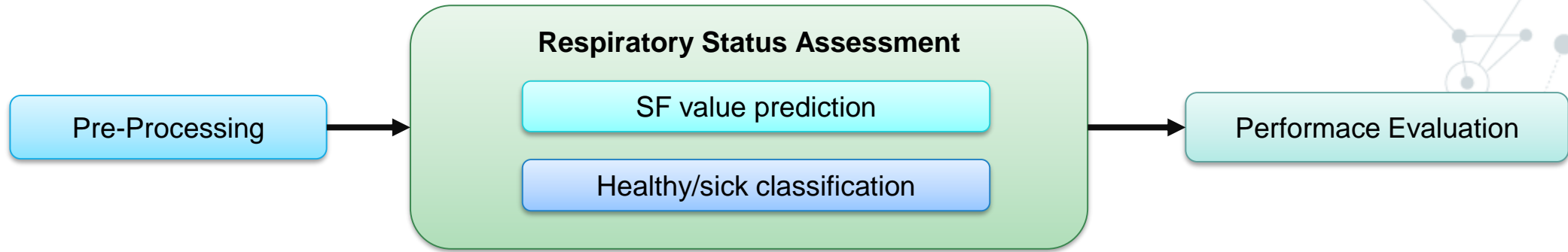
<sup>4</sup>M. Palacio et al. "Prediction of neonatal respiratory morbidity by quantitative ultrasound lung texture analysis: a multicenter study," American journal of obstetrics and gynecology.

<sup>5</sup>P. Chen et al. "A preliminary study to quantitatively evaluate the development of maturation degree for fetal lung based on transfer learning deep model from ultrasound images," International Journal of Computer Assisted Radiology and Surgery.

<sup>6</sup>X. P. Burgos-Artizzu et al. "Evaluation of an improved tool for non-invasive prediction of neonatal respiratory morbidity based on fully automated fetal lung ultrasound analysis," Scientific reports

<sup>7</sup>F. Raimondi et al. "Visual assessment versus computer-assisted gray scale analysis in the ultrasound evaluation of neonatal respiratory status," PLOS ONE

# Methodology



Pre processing

→ Lung US images are prepared to feed into the involved CNN

Respiratory Status Assessment

SF value prediction

→ The CNN is directly trained to predict SF value

Healthy/sick classification

→ The CNN is trained with class labels (Healthy, Sick)

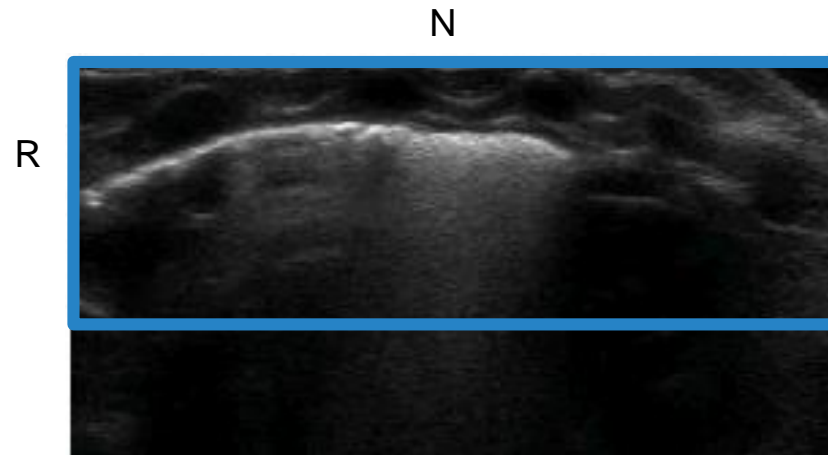
Performance Evaluation

→ Correlation between CNN output and SF value is evaluated

# Pre-Processing

## Data preparation

- Images are normalized in 0-1 range and resized to have the same horizontal resolution (N)
- The first R rows are retained according to the CNN input size
- The obtained rectangular-shaped (RxN):
  - ✓ always includes the pleural line and part of the lung below it
  - ✓ allows the network to process the whole US from left to right without discarding relevant regions
  - ✓ does not include the bottom region of the US images, which carries no useful information



## Data augmentation:

- ✓ Random Horizontal Flip
- ✓ Random Rotation in the range  $[-10, 10]$
- ✓ Contrast and brightness change
- ✗ Vertical flip results in non-sense images
- ✗ Stronger rotations result in unnatural images

# Respiratory Status Assessment

## SF value prediction

- Train the CNN to directly predict the SF value with regression loss (mean squared error)
- SR value is normalized in the unity range for better training stability.
- Since distinguishing between two very high values (e.g. SF above 450) is useless, SF value is clipped to 450.
  - SF above 450 represents either an healthy or a completely healed patient

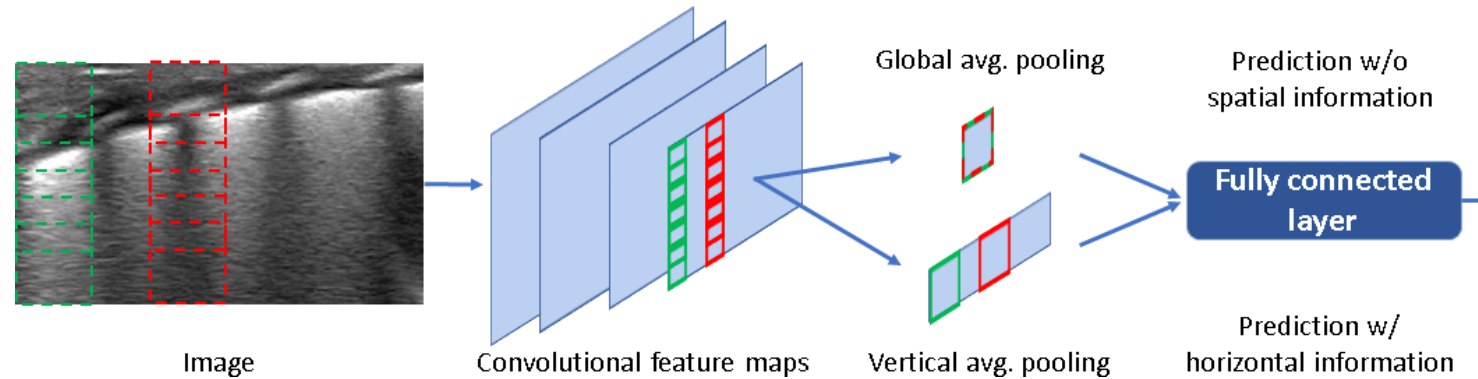
## Healthy/Sick classification

- Train the CNN with class labels (i.e healthy or sick) that will be predicted with a certain confidence:
  - The confidence can be regarded as class probability
- SF above 450 is used to distinguish between healthy and sick images

# Advanced Training Strategy

## CNN architecture variation

- Preserve the horizontal position of the extracted features to avoid mixing up visually different regions of the US, e.g. correct US acquisition (green) and shadow effect due to ribs (red)
- Replace the Global Average Pooling with a Vertical Average Pooling



## Curriculum Learning

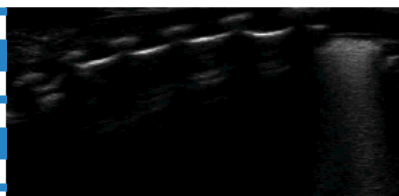
- The training procedure consists of two phases:
  - Train the CNN with **easy** example
  - Add **hard** or **borderline** samples in a second step



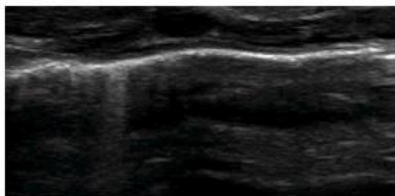
# Experimental Setup

## Dataset

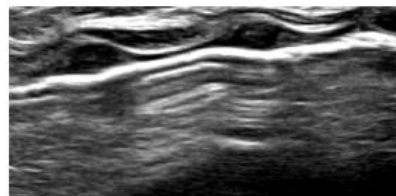
Disease	Number of		Patients per center		
	patient	videos	Naples	Milan	Florence
None	43	328	23	10	10
RDS	30	727	11	8	11
TTN	13	211	13	-	-
Tot.	86	1266	47	18	21



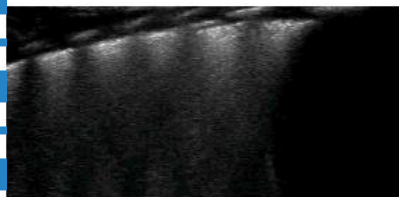
(a) Healthy (Naples)



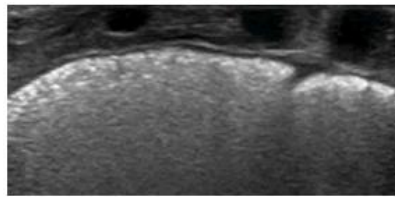
(d) Healthy (Florence)



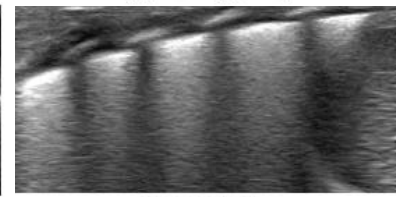
(g) Healthy (Milan)



(c) RDS (Naples)



(f) RDS (Florence)



(i) RDS (Milan)

Videos are acquired with several US instruments

From each video:

- 10 evenly spaced frames are selected during training
- 6 evenly spaced frames are selected during performance evaluation

## Involved CNN:

- AlexNet<sup>8</sup>
- ResNet34<sup>9</sup>
- EfficientNet-B0<sup>10</sup>
- EfficientNet-B1<sup>10</sup>
- EfficientNet-B2<sup>10</sup>

<sup>8</sup>A. Krizhevsky et al, "Imagenet classification with deep convolutional neural networks"

<sup>9</sup>K. He et al. "Deep residual learning for image recognition"

<sup>10</sup>M. Tan et al. "Efficientnet: Rethinking model scaling for convolutional neural networks"

## Performance evaluation

### • SF value prediction

- Mean absolute percentage of Error (MAPE)
- Spearman's rank correlation between predicted SF and SF value

### • Healthy/Sick classification

- Accuracy (ACC)
- Spearman's rank correlation between prediction probability and SF value

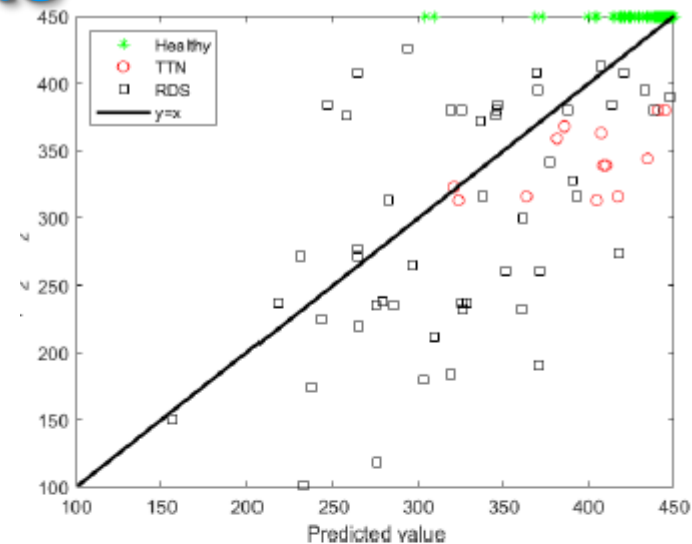


# SF Value Prediction - Results

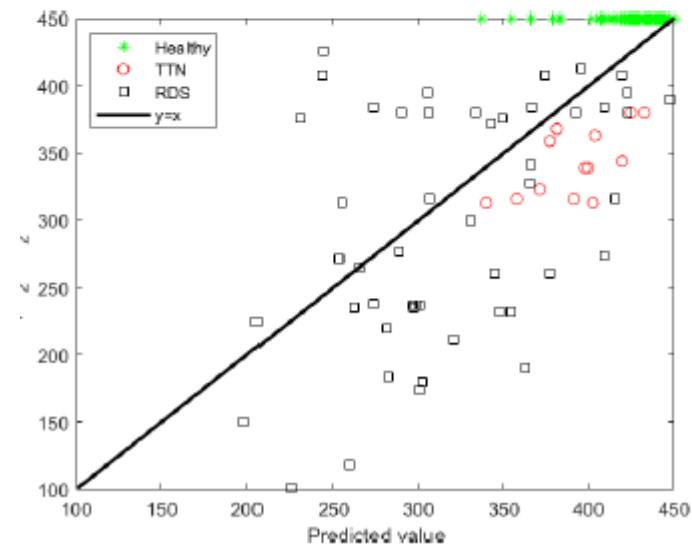
TABLE III

REGRESSION RESULTS OF THE CONSIDERED BASELINES WITH DIFFERENT AUGMENTATIONS. FROM TOP TO BOTTOM WE REPORT THE RESULTS WITHOUT ANY AUGMENTATION AND BY ADDING THE FOLLOWING OPERATIONS, CONSECUTIVELY: RANDOM HORIZONTAL FLIP, RANDOM ROTATION IN THE RANGE  $[-10^\circ, +10^\circ]$ , RANDOM BRIGHTNESS AND OR CONTRAST VARIATION IN THE RANGE  $[-25\%, +25\%]$ .

Network	Input size	Augmentation	Correlation			MAPE		
			frame	video	session	frame	video	session
AlexNet	224×461	None	0.6678	0.6857	0.7371	0.1472	0.1430	0.1368
ResNet34	224×461	None	0.6291	0.6812	0.7398	0.1614	0.1465	0.1339
EfficientNet-B0	224×461	None	0.6383	0.6739	0.7357	0.1521	0.1399	0.1276
EfficientNet-B1	240×461	None	0.6735	0.7024	0.7487	0.1428	0.1345	<b>0.1250</b>
EfficientNet-B2	260×461	None	0.6754	0.7033	0.7630	0.1474	0.1402	0.1298
AlexNet	224×461	hor. flip	0.6587	0.6772	0.7263	0.1474	0.1454	0.1420
ResNet34	224×461	hor. flip	0.6504	0.6969	0.7556	0.1453	0.1414	0.1355
EfficientNet-B0	224×461	hor. flip	0.5857	0.6119	0.6653	0.1653	0.1609	0.1552
EfficientNet-B1	240×461	hor. flip	0.6645	<b>0.6998</b>	0.7637	<b>0.1377</b>	<b>0.1338</b>	0.1282
EfficientNet-B2	260×461	hor. flip	0.6620	0.6905	0.7576	0.1424	0.1389	0.1317
AlexNet	224×461	hor. flip, $\pm 10^\circ$ rot.	0.6644	0.6804	0.7328	0.1506	0.1492	0.1442
ResNet34	224×461	hor. flip, $\pm 10^\circ$ rot.	0.6621	0.6963	<b>0.7662</b>	0.1428	0.1389	0.1329
EfficientNet-B0	224×461	hor. flip, $\pm 10^\circ$ rot.	0.5994	0.6349	0.7070	0.1669	0.1620	0.1557
EfficientNet-B1	240×461	hor. flip, $\pm 10^\circ$ rot.	0.6642	0.6935	0.7534	0.1448	0.1419	0.1359
EfficientNet-B2	260×461	hor. flip, $\pm 10^\circ$ rot.	0.6661	0.6953	0.7592	0.1441	0.1408	0.1326
AlexNet	224×461	hor. flip, $\pm 10^\circ$ rot., bri./cont. adj	<b>0.6695</b>	0.6889	0.7442	0.1498	0.1481	0.1447
ResNet34	224×461	hor. flip, $\pm 10^\circ$ rot., bri./cont. adj	0.6649	0.6959	0.7623	0.1391	0.1349	0.1282
EfficientNet-B0	224×461	hor. flip, $\pm 10^\circ$ rot., bri./cont. adj	0.6067	0.6471	0.7176	0.1668	0.1619	0.1555
EfficientNet-B1	240×461	hor. flip, $\pm 10^\circ$ rot., bri./cont. adj	0.6563	0.6847	0.7416	0.1457	0.1429	0.1374
EfficientNet-B2	260×461	hor. flip, $\pm 10^\circ$ rot., bri./cont. adj	0.6638	0.6916	0.7577	0.1445	0.1415	0.1338



(a)



(b)

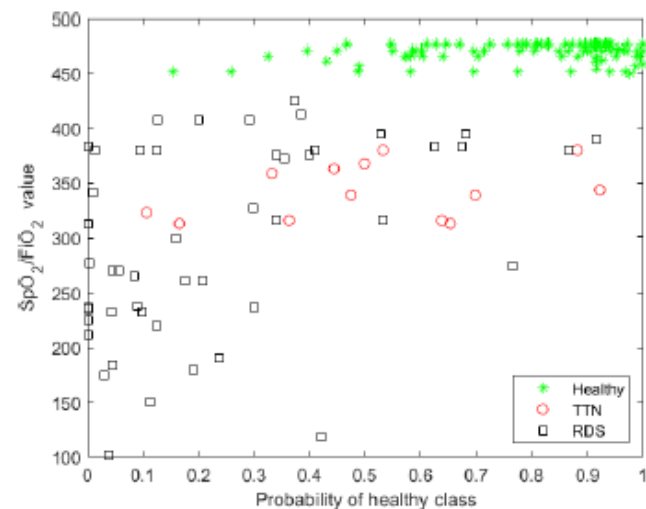
Fig. 3. Scatter plots of the predicted score with EfficientNet-B1 (top) and ResNet34 (bottom) architectures trained respectively without and with the random rotation.

# Healthy/Sick classification - Results

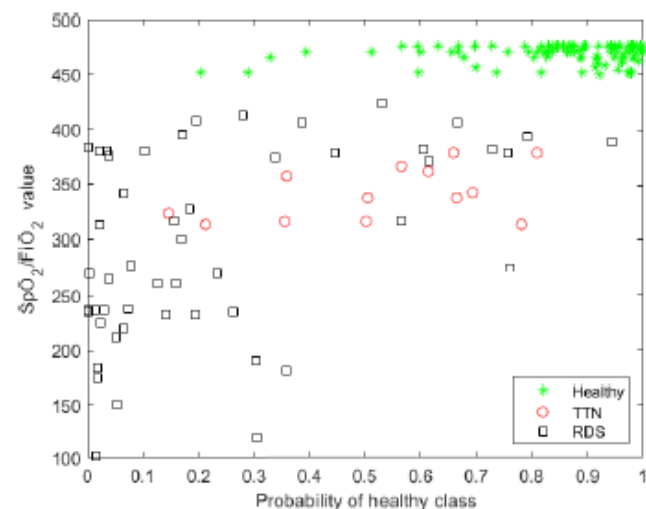
TABLE IV

BINARY CLASSIFICATION RESULTS OF THE CONSIDERED BASELINES WITH DIFFERENT AUGMENTATIONS. FROM TOP TO BOTTOM WE REPORT THE RESULTS WITHOUT ANY AUGMENTATION AND BY ADDING THE FOLLOWING OPERATIONS, CONSECUTIVELY: RANDOM HORIZONTAL FLIP, RANDOM ROTATION IN THE RANGE  $[-10^\circ, +10^\circ]$ , RANDOM BRIGHTNESS AND OR CONTRAST VARIATION IN THE RANGE  $[-25\%, +25\%]$ .

Network	Input size	Augmentation	Correlation			Accuracy		
			frame	video	session	frame	video	session
AlexNet	224×461	None	0.6586	0.6749	0.7518	0.8121	0.8245	0.8461
ResNet34	224×461	None	0.6507	0.6830	0.7562	0.8129	0.8229	0.8397
EfficientNet-B0	224×461	None	0.6536	0.6794	0.7463	0.8159	0.8316	0.8461
EfficientNet-B1	240×461	None	0.6647	0.6928	0.7578	0.8214	0.8332	0.8653
EfficientNet-B2	260×461	None	0.6471	0.6687	0.7353	0.8166	0.8340	0.8654
AlexNet	224×461	hor. flip	0.6593	0.6729	0.7458	0.8054	0.8166	0.8462
ResNet34	224×461	hor. flip	0.6414	0.6701	0.7526	0.8096	0.8182	0.8397
EfficientNet-B0	224×461	hor. flip	0.6425	0.6641	0.7351	0.8141	0.8190	0.8397
EfficientNet-B1	240×461	hor. flip	0.6461	0.6752	0.7533	0.8194	0.8356	0.8718
EfficientNet-B2	260×461	hor. flip	0.6390	0.6690	0.7431	0.8152	0.8237	0.8397
AlexNet	224×461	hor. flip, $\pm 10^\circ$ rot.	0.6485	0.6658	0.7363	0.8124	0.8229	0.8526
ResNet34	224×461	hor. flip, $\pm 10^\circ$ rot.	0.6602	0.6869	0.7546	0.8248	<b>0.8387</b>	<b>0.8782</b>
EfficientNet-B0	224×461	hor. flip, $\pm 10^\circ$ rot.	0.6696	0.6883	0.7543	<b>0.8292</b>	0.8364	0.8526
EfficientNet-B1	240×461	hor. flip, $\pm 10^\circ$ rot.	0.6539	0.6794	0.7540	0.8156	0.8356	0.8462
EfficientNet-B2	260×461	hor. flip, $\pm 10^\circ$ rot.	0.6378	0.6634	0.7264	0.8123	0.8245	0.8590
AlexNet	224×461	hor. flip, $\pm 10^\circ$ rot., bri./cont. adj	0.6557	0.6690	0.7310	0.8061	0.8206	0.8590
ResNet34	224×461	hor. flip, $\pm 10^\circ$ rot., bri./cont. adj	<b>0.6777</b>	<b>0.7030</b>	<b>0.7782</b>	0.8208	<b>0.8387</b>	0.8526
EfficientNet-B0	224×461	hor. flip, $\pm 10^\circ$ rot., bri./cont. adj	0.6581	0.6819	0.7586	0.8249	0.8379	0.8590
EfficientNet-B1	240×461	hor. flip, $\pm 10^\circ$ rot., bri./cont. adj	0.6592	0.6828	0.7564	0.8138	0.8340	0.8590
EfficientNet-B2	260×461	hor. flip, $\pm 10^\circ$ rot., bri./cont. adj	0.6620	0.6846	0.7501	0.8104	0.8316	0.8718



(a)



(b)

Fig. 4. Scatter plots of the predicted score with ResNet34 architecture trained with classification-based strategy respectively without (top) and with (bottom) brightness/contrast random adjustment.

# Advanced Training Strategies - Results

TABLE V

RESULTS OF THE BEST PERFORMING NETWORKS WITH CURRICULUM LEARNING AND HORIZONTAL POSITION INFORMATION PRESERVING.

Train mode	Network	Advanced training	Correlation			MAPE or Accuracy		
			frame	video	session	frame	video	session
Regression	ResNet34	hor. flip position	0.6734	0.6778	0.7440	0.1681	<b>0.1427</b>	<b>0.1344</b>
	EfficientNet-B1	hor. flip position	0.6361	0.6754	0.7505	<b>0.1511</b>	0.1475	0.1395
Classification	ResNet34	hor. flip position	0.6766	<b>0.7051</b>	<b>0.7821</b>	0.8179	0.8324	<b>0.8718</b>
	EfficientNet-B1	hor. flip position	0.6459	0.6747	0.7608	0.8092	0.8261	0.8333
	ResNet34	Curriculum Learning	<b>0.6780</b>	0.6995	0.7604	<b>0.8195</b>	0.8348	0.8654
	EfficientNet-B1	Curriculum Learning	0.6645	0.6852	0.7600	0.8161	<b>0.8616</b>	0.8590

- Correlation between **LUS score assigned by humans expert<sup>7</sup>** and SF value: **0.8259**

<sup>7</sup>F. Raimondi et al. "Visual assessment versus computer-assisted gray scale analysis in the ultrasound evaluation of neonatal respiratory status," PLOS ONE

# Conclusion

- Results show that ResNet34 trained for binary classification achieves the best performance in terms of correlation with the selected reference marker
- The correlation further improves by modifying the CNN architecture in order to take into account the horizontal position of the extracted convolutional networks
- It is worth observing that the proposed approach performs comparably with the human operator (+4.4%)

# Future Work

- Future research will be devoted to:
  - enlarge the dataset including data from other medical centers
  - improve the training strategy by exploiting the temporal information of the lung US videos